Enhanced external radiative efficiency for 20.8% efficient single-junction GaInP solar cells

J. F. Geisz, M. A. Steiner, I. García, S. R. Kurtz, and D. J. Friedman

Citation: Appl. Phys. Lett. **103**, 041118 (2013); doi: 10.1063/1.4816837
View online: http://dx.doi.org/10.1063/1.4816837
View Table of Contents: http://apl.aip.org/resource/1/APPLAB/v103/i4
Published by the AIP Publishing LLC.

Enhanced external radiative efficiency for 20.8% efficient single-junction GaInP solar cells

J. F. Geisz,[1] M. A. Steiner,[1] I. García,[1,2] S. R. Kurtz,[1] and D. J. Friedman[1]
[1]*National Renewable Energy Laboratory, Golden, Colorado 80401, USA*
[2]*Instituto de Energía Solar, Universidad Politécnica de Madrid, Avda Complutense s/n, 28040 Madrid, Spain*

(Received 28 June 2013; accepted 12 July 2013; published online 25 July 2013)

We demonstrate 1.81 eV GaInP solar cells approaching the Shockley-Queisser limit with 20.8% solar conversion efficiency, 8% external radiative efficiency, and 80–90% internal radiative efficiency at one-sun AM1.5 global conditions. Optically enhanced voltage through photon recycling that improves light extraction was achieved using a back metal reflector. This optical enhancement was realized at one-sun currents when the non-radiative Sah-Noyce-Shockley junction recombination current was reduced by placing the junction at the back of the cell in a higher band gap AlGaInP layer. Electroluminescence and dark current-voltage measurements show the separate effects of optical management and non-radiative dark current reduction. © *2013 AIP Publishing LLC*. [http://dx.doi.org/10.1063/1.4816837]

Recently, the efficiency of single-junction GaAs solar cells, long assumed to have reached its practical limit, has increased significantly through the careful management of optical emission.[1–3] In particular, the open-circuit voltage (V_{oc}) and the voltage at the maximum power point (V_{mp}) are improved through increased photon recycling using a highly reflective mirror at the back of the device, which prevents parasitic absorption of emitted photons in the substrate. In principle, this voltage boost through optical management can be applied to any solar cell material that has a high probability of minority carrier recombination through radiative pathways. In fact, each junction of a multijunction solar cell could be boosted in this way *if* the emitted photons from each junction can be confined to reabsorption only in that emitting junction *and* carriers within that junction have a high probability of radiative recombination.[4] The upper-most junction of most III-V multijunction solar cells is composed of $Ga_{0.5}In_{0.5}P$, a direct band gap semiconductor with demonstrated high emission efficiency in light-emitting diodes. In this Letter, we demonstrate how $Ga_{0.5}In_{0.5}P$ solar cells can be enhanced through improvements in junction design to reduce non-radiative Sah-Noyce-Shockley (SNS) junction recombination, combined with improved optical management of emitted light. We use external radiative efficiency as the primary figure of merit to compare solar cells. We demonstrate record high external radiative efficiency and solar cell conversion efficiency from single-junction GaInP solar cells.

The bandgap energy (E_g) of $Ga_{0.5}In_{0.5}P$ can vary due to CuPt ordering,[5] making the V_{oc} by itself an imperfect figure of merit for the material. The difference between E_g and V_{oc} has been accepted as an empirical figure of merit to compare the quality of solar cells of different materials[6] and a solar cell's voltage is generally considered high when $W_{oc} \equiv (\frac{E_g}{q} - V_{oc}) < 0.4\,\mathrm{V}$, where q is the elementary charge. The external radiative emission efficiency (η_{ext}) of a solar cell at open-circuit is a much better figure of merit[7,8] because it characterizes how closely the V_{oc} has approached the Shockley-Queisser[9] (SQ) detailed balance or radiative limit (V_{oc}^{rad})

$$V_{oc} = V_{oc}^{rad} + \frac{kT}{q}\ln(\eta_{ext}(J_{sc})), \tag{1}$$

where k is the Boltzmann constant and T is the solar cell temperature. But the solar cell efficiency is actually determined at the maximum power point rather than open-circuit, so it is preferable to characterize η_{ext} as a function of the injection current density ($J_{inj} \equiv J + J_{sc}$), where the short-circuit current density (J_{sc}) is approximately the photocurrent and the total current density (J) is taken as negative in the power-producing quadrant. The voltage at any injection current density is directly related to η_{ext} by[7]

$$\eta_{ext}(J_{inj}) \approx \frac{J_0^{rad}}{J_{inj}}\exp\left(\frac{qV}{kT}\right) \tag{2}$$

for $J_{inj} \gg J_0^{rad}$, where the Shockley-Queisser dark current density of a particular device in the radiative limit, J_0^{rad}, can be calculated from an integration of the product of the measured solar cell external quantum efficiency (EQE) and the black body emission spectrum at the device temperature.[7,10] Equation (2) provides a reciprocal relation between electrical dark IV measurements and electroluminescence (EL) measurements in the dark. Because the voltage determined from EL is the actual junction voltage, this method is useful to remove the effects of series resistance at high currents and can also be used to determine the individual subcell voltages of multijunction solar cells.[11] We characterize the dark IV and $\eta_{ext}(J_{inj})$ here for a variety of GaInP solar cells to demonstrate the impacts of the optical and electronic structure on $\eta_{ext}(J_{inj})$ and thus the solar cell voltage.

The injected current of III-V solar cells is dominated by two recombination mechanisms with different voltage dependencies that can be characterized by a two-diode model

$$J_{inj} = J_{01}\left(e^{\frac{qV}{kT}} - 1\right) + J_{0m}\left(e^{\frac{qV}{mkT}} - 1\right). \tag{3}$$

The first, "n = 1" term describes diffusion or bulk recombination that includes band-to-band radiative recombination in

the bulk regions that gives rise to photon emission, and the second term describes non-radiative Shockley-Read-Hall recombination that occurs via deep-level states within the junction and perimeter space-charge regions, as described by SNS.[12,13] The ideality factor of the SNS contribution (m) is generally greater than 1. The SNS ideality factor for many materials is typically $m \sim 2$, but for GaInP is often observed to be $m \sim 1.5$–2. We combine Eqs. (2) and (3) to calculate $\eta_{ext}(J_{inj})$ in the context of this model. At high current densities, the $n = 1$ behavior dominates and the radiative efficiency saturates to a constant value of $\eta_{ext}^{bulk}(J_{inj}) \approx J_0^{rad}/J_{01}$, but at low current densities, the radiative efficiency drops off as the current density decreases: $\eta_{ext}^{SNS}(J_{inj}) \approx \frac{J_0^{rad}}{J_{0m}^{m}} J_{inj}^{(m-1)}$. The current density where these two contributions are equal is given by

$$J_{knee} = 2J_{01}\left[\frac{J_{0m}}{J_{01}}\right]^{\left(\frac{m}{m-1}\right)} \tag{4}$$

and is at the location of an obvious knee in the $\eta_{ext}(J_{inj})$ data that separates the SNS-dominated from the bulk-dominated regions.[14]

The solar cells studied here were n-on-p structures with a ~20 nm Se-doped n-type $Al_{0.5}In_{0.5}P$ window layer and a Zn-doped p-type $Al_{0.25}Ga_{0.25}In_{0.5}P$ back surface field (BSF) layer. The total GaInP thickness of all devices was nominally 1 μm. The traditional structure[15,16] consists of a very thin AlInP window layer, a thin (~0.1 μm) highly n-type ($\sim 2\times10^{18}$cm^{-3}) GaInP emitter layer, a 1-μm-thick lightly p-type GaInP base layer, and a high-E_g BSF (typically AlGaAs or AlGaInP). Here, we compare this *traditional* electronic structure with a *rear heterojunction* structure that consists of a 1-μm-thick emitter ($n \sim 5\times10^{17}$cm^{-3}) and a p-type GaInP base < 40 nm thick so that the $Al_{0.25}Ga_{0.25}In_{0.5}P$ BSF may be acting as the base. The device structures are compared in Fig. 1. The thickness and location of the depletion region (shown as yellow shading) are very different in the two electronic structures. These devices were grown by atmospheric-pressure metal-organic vapor phase epitaxy (MOVPE) as described elsewhere,[17] on single-crystal (001) GaAs substrates miscut by 2° and at growth conditions that give rise to a high degree of CuPt ordering in the GaInP. A MgF_2/ZnS antireflection coating was applied. Solar cells were grown either in an *upright* configuration from the back toward the sun-side or in an *inverted* configuration starting with a GaInP etch stop and the sun-side portion of the cell, growing toward the back of the solar cell. Inverted solar cells were processed using the inverted metamorphic multijunction (IMM) process.[18] The back metal contact in the inverted structures provides an effective optical back reflector to internally emitted band edge photons for enhanced photon recycling.[1,2] The 200-nm carbon-doped $Al_{0.5}Ga_{0.5}As$ back contact layer is transparent to the emitted photons. In some inverted structures, we intentionally reduced the back reflectance by adding an absorbing $Al_{0.2}Ga_{0.8}As$ contact layer with varying thickness. The GaAs substrate in upright structures effectively absorbs all of the emitted photons that enter it, thereby providing very poor back reflectance.

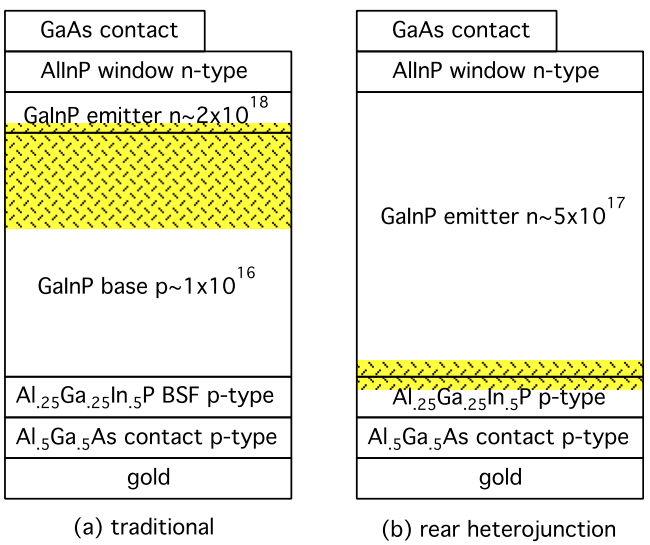

FIG. 1. Schematic of electronic structures: (a) traditional and (b) rear heterojunction. The depletion regions are shaded (yellow online).

The η_{ext} of solar cells dominated by bulk recombination can be related to the optical structure through an effective internal radiative efficiency[1] (η_{int})

$$\eta_{ext} = \frac{\eta_{int}\overline{P_{esc}}}{1 - \eta_{int}\overline{P_{abs}}}, \tag{5}$$

where $\overline{P_{esc}}$ represents the average probability that an internally emitted photon escapes out the front before being reabsorbed, and $\overline{P_{abs}}$ is the average probability of reabsorption. We calculate these probabilities from the device structures:[1] for the upright GaInP solar cells with an absorbing GaAs substrate, we calculate $\overline{P_{esc}} = 1.53\%$ and $\overline{P_{abs}} = 60.2\%$; for the inverted GaInP solar cells with a good gold back reflector, we calculate $\overline{P_{esc}} = 2.44\%$ and $\overline{P_{abs}} = 90.1\%$. The resulting maximum theoretical η_{ext} that can be achieved assuming $\eta_{int} = 1$ are therefore 3.9% and 24.6% for the upright and high-reflectance inverted GaInP solar cells, respectively.

Solar cell performance was characterized by EQE and current-voltage (IV) measurements in the dark and under a Xe solar simulator using a matched reference cell and spectral mismatch correction.[19] Spectrally resolved EL of the solar cells was measured in the dark over a range of injection current densities. The total external radiative flux (J_{em}) in units of current density was estimated from measurements of light captured over a small solid angle, Ω_{FO}, by a fiber optic bundle with numerical aperture 0.22 placed about 5 mm from the device and coupled to a Spectral Evolution spectroradiometer. We assume that the angular emission pattern from the device is similar to the calibrated broadband light that is reflected from a nearly Lambertian Spectralon® sample placed in the position of the solar cell.

$$J_{em} \approx \frac{q}{K}\int \frac{\phi_{cal}(\lambda)}{\phi_{cal}^{\Omega_{FO}}(\lambda)}\phi_{em}^{\Omega_{FO}}(\lambda)d\lambda, \tag{6}$$

where $\phi_{em}^{\Omega_{FO}}(\lambda)$ is the EL spectrum of the device collected at the fiber optic, $\phi_{cal}(\lambda)$ is the photon flux of a calibrated broadband light, and $\phi_{cal}^{\Omega_{FO}}(\lambda)$ is the broadband spectrum reflected from the Spectralon and collected at the fiber optic

during calibration. This wavelength-dependent calibration provides a good estimate of J_{em} for a wide range of wavelengths. The wavelength-independent constant, K, represents a geometric factor that takes into consideration that the area of the device may not be infinite relative to the field of view of the fiber optic and can also correct for other small uncertainties in the calibration such as an actual reflectance of the Spectralon less than unity. The external radiative emission efficiency is defined by $\eta_{ext}(J_{inj}) \equiv J_{em}(J_{inj})/J_{inj}$. Dark IV measurements were made at the same time as the EL measurements. The junction voltage was calculated from the measured EL using Eq. (2). The constant K in Eq. (6) was determined precisely for each measurement by matching the measured dark IV curves with the dark IV curves calculated from EL in a region in which series resistance was negligible and a strong EL signal-to-noise was achieved. K ranged from 0.78 to 1.0 for these 0.25 cm^2 devices and fiber optic placement. Measured and EL-calculated dark currents are plotted in Fig. 2(a). The $\eta_{ext}(J_{inj})$ measured by EL and calculated from the dark IV measurements using Eq. (2) are plotted in Fig. 2(b). The EL method is especially useful at high current densities where series resistance dominates electrical IV measurements. The electrical IV measurement is particularly useful at low current densities when the light emission is below the signal-to-noise level. For clarity, we have only plotted the electrical measurement up to the point at which the series resistance begins to dominate.

The data in Fig. 2 compare the dark IV and $\eta_{ext}(J_{inj})$ of GaInP solar cells with traditional vs. rear heterojunction electrical designs and reflective (inverted) vs. absorbing (upright) optical designs. At high enough current densities, the device should eventually be dominated by $n = 1$ bulk recombination where η_{ext} saturates to a constant value. η_{ext} at the highest current densities is much higher in the inverted devices with excellent back reflectors than in the upright devices with absorbing GaAs substrates. These maximum values are slightly below the theoretical predictions for $\eta_{int} = 1$. At low current densities, the emission from all devices drops off dramatically because SNS recombination dominates. But at intermediate current densities, the rear heterojunction designs (both inverted and upright) remain relatively constant for current densities well below one-sun photocurrents (shown as a yellow bar). Indeed, the transition between SNS-dominated and bulk-dominated recombination (i.e., J_{knee} indicated with vertical arrows in Fig. 2(b)) is several orders of magnitude lower in the rear heterojunction devices than the traditional structures. The V_{oc} can be determined at the one-sun current density from the dark IV curve in Fig. 2(a) or η_{ext} in Fig. 2(b). At this current density, we observe an order of magnitude greater η_{ext} (and corresponding high V_{oc}) in the device with a back metal reflector and the rear heterojunction design than any other device structure.

The solar cell performance characteristics of these GaInP devices and others optimized for one-sun global measurements are summarized in Table I. All devices perform quite favorably compared to previous reports in the literature. Takamoto *et al.* reported a 17.4% efficiency with a V_{oc} of 1.39 V for a GaInP solar cell (E_g not reported).[20] Olson *et al.* reported V_{oc} varying from 1.35 to 1.42 V as E_g was systematically varied from 1.80 to 1.89 eV through ordering, giving a minimum W_{oc} of 0.45 V.[5] The best solar cell reported here has a confirmed solar cell efficiency of 20.8% at AM1.5 global conditions with a W_{oc} of 0.35 V. The external radiative efficiency at one-sun is over 8% with an effective internal radiative efficiency over 80%. This V_{oc} is within 63 mV of the SQ radiative limit and our modeling indicates that this planar geometry with a reflector can only approach the SQ limit to within 38 mV. Without a back reflector, the model predicts that a perfect (i.e., $\eta_{int} = 1$) GaInP solar cell can only approach the SQ limit to within 85 mV.

Equation (5) indicates that photon recycling is important only when η_{int} is relatively large, which can only occur when bulk $n = 1$ recombination dominates. In order to realize optical enhancement to the V_{oc} and efficiency of GaInP solar cells, it is therefore critical to reduce the SNS recombination so that $J_{knee} < J_{inj}$ at these conditions. In general, both J_{01} and J_{0m} decrease with increasing E_g, but the ratio J_{0m}/J_{01} increases with increasing E_g.[21] It is therefore more challenging to fabricate high bandgap solar cells that are dominated by bulk recombination at low current densities than lower bandgap solar cells. Ragay *et al.* showed that, since the regions where these two recombination mechanisms take

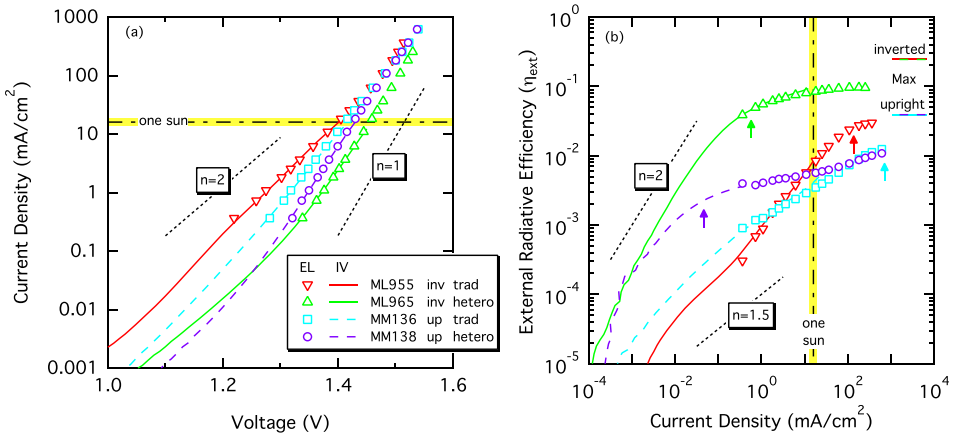

FIG. 2. Electroluminescence (markers) and electrical dark IV (lines) measurements presented as (a) IV curves and (b) external radiative efficiency as a function of dark current density. Typical one-sun current density of 16 mA/cm^2 is indicated with dotted-dashed line (highlighted in yellow online). The black dotted lines show diode dependencies with various ideality factors. The maximum theoretical η_{ext} for the structure with and without a back metal reflector are shown at the right of (b). The transitions from SNS- to bulk-dominated recombination (J_{knee}) are indicated with vertical arrows in (b).

TABLE I. Summary of solar cell measurements.

Device ID	Growth direction	Parasitic absorber	Junction placement	V_{oc} (V)	J_{sc} (mA/cm^2)	FF (%)	Eff (%)	E_g (eV)	W_{oc} (V)	V_{oc}^{rad} (V)	J_0^{rad} (mA/cm^2)	η_{ext} (J_{sc}) (%)	η_{int} (J_{sc}) (%)
MM136	Upright	Substrate	Traditional	1.406	14.8[a]	88.3	18.4	1.843	0.44	1.556	7.18×10^{-26}	0.32	19
MM138	Upright	Substrate	Rear hetero	1.413	11.5[a]	88.1	14.3	1.843	0.43	1.550	6.84×10^{-26}	0.53	30
ML955	Inverted	None	Traditional	1.392	15.8[a]	85.8	18.9	1.810	0.42	1.524	2.71×10^{-25}	0.75	25
ML965	Inverted	None	Rear hetero	1.452	15.8[a]	89.4	20.5	1.805	0.35	1.518	3.47×10^{-25}	8.29	85
MM083	Inverted	None	Rear hetero	1.458	16.0[b]	88.7	20.7	1.810	0.35	1.521	3.20×10^{-25}	8.71	86
MM081	Inverted	None	Rear hetero	1.455	16.0[b]	89.3	20.8	1.810	0.35	1.522	3.01×10^{-25}	7.64	83

[a]Measured under G173 AM1.5 Direct conditions (with busbar area removed), not independently confirmed.
[b]Measured under G173 AM1.5 Global conditions and independently confirmed by NREL measurements team.

place are spatially separated, a higher bandgap material could be placed within the depletion region to reduce J_{0m} and thus increase V_{oc} if the device is dominated by SNS recombination at the operating current.[22] While they demonstrated increased V_{oc} in GaAs solar cells, the barriers to carrier collection that resulted from inserting AlGaAs into the traditional location of the depletion region minimized the impact on total efficiency. The rear heterojunction structure used in our work places the depletion region partially within the high-E_g $Al_{0.25}Ga_{0.25}In_{0.5}P$ layer at the back of the device, effectively reducing J_{0m} and, thus J_{knee}, without necessarily reducing the density of deep-level states within the junction. Since most of the high energy photons from the solar spectrum are absorbed before they reach the $Al_{0.25}Ga_{0.25}In_{0.5}P$ layer and photons closer to the GaInP band edge are not absorbed there, there is very little photon absorption within the $Al_{0.25}Ga_{0.25}In_{0.5}P$ layer. Therefore, even if the $Al_{0.25}Ga_{0.25}In_{0.5}P$ is acting as the base layer, minority carrier passivation at the back (i.e., BSF) is not required unless the cell is very thin. If the high-E_g heterojunction were at the front of the device, significant carrier generation would take place in this layer.

The V_{oc} and $\eta_{ext}(J_{sc})$ of these devices and others with intermediate back reflectances are plotted in Fig. 3, along with the predictions of Eqs. (5) and (1) for various values of η_{int}. As noted above, the average back reflectance was reduced in some inverted devices by growing a parasitic absorbing $Al_{0.2}Ga_{0.8}As$ layer between the junction and the back gold contact. The figure shows that V_{oc} and η_{ext} increase with reflectivity when using the rear heterojunction design. Comparing the results with the model, η_{int} at one-sun photocurrents appears to be only about 20% for the traditional design, but increases to 80–90% for the rear heterojunction design in the inverted devices. Only a modest increase in η_{int} was observed in upright structures when going from the traditional to rear heterojunction design even though Fig. 2(b) indicates that the rear heterojunction device is now bulk-recombination-dominated at one-sun. In principle, there should be little difference in the optical structure between the inverted device with a thick parasitic absorbing layer and the upright structure with an absorbing GaAs substrate, but the bulk recombination in the thick emitter of the upright device may be primarily non-radiative due to problematic Zn diffusion[17,23] that may depend on the growth direction.[24]

Reduced J_{sc} and EQE in the upright device with a rear heterojunction structure indicate that the diffusion length in the emitter is less than 1 μm. This is consistent with previous literature[20] that concluded that the traditional thin-emitter design is optimal. It is therefore noteworthy that the inverted devices do not seem to show a reduced J_{sc}. Thus, the material quality of the n-type GaInP emitter appears to be improved when the solar cell is grown in the inverted configuration. This may again be the result of differences in Zn diffusion depending on the growth direction, but will require further investigation. In any case, the ability to use this relatively thick emitter layer in the inverted devices also results in a lower sheet resistance of ~150 Ω/sq than in the traditional thin emitter devices (>400 Ω/sq).

In summary, we have increased the external radiative efficiency of GaInP solar cells by an order of magnitude, thereby approaching the SQ limit. The current density at which the recombination transitions from SNS-dominated to bulk-dominated was reduced below one-sun levels by moving the junction into a high-Eg $Al_{0.25}Ga_{0.25}In_{0.5}P$ layer at the back of the device. This rear heterojunction design can also

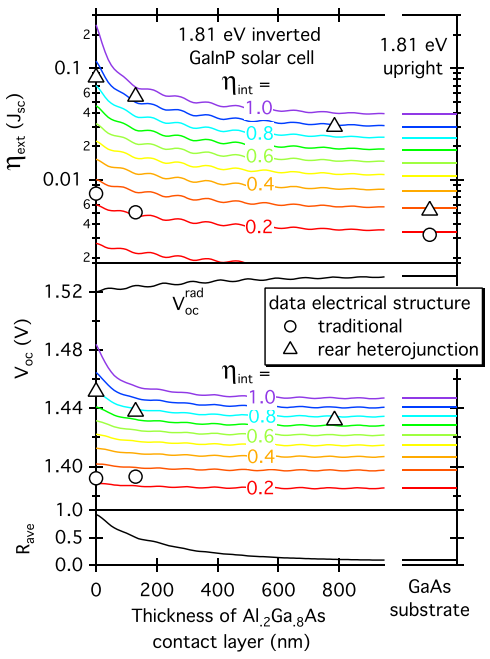

FIG. 3. $\eta_{ext}(J_{sc})$, V_{oc} and angle-averaged back reflectance (R_{ave}) as a function of $Al_{0.2}Ga_{0.8}As$ parasitic absorbing layer thickness in inverted solar cells. Upright cells with a thick GaAs substrate are shown on the right. Triangles show data for the rear heterojunction electrical design and circles show data for the traditional electrical design. The lines show the predictions of Eqs. (5) and (1). The V_{oc} of the upright structures are not shown because E_g for these was significantly higher.

result in significant voltage improvement in inverted multijunction solar cells. Further voltage improvements could be realized in inverted multijunction solar cells if an effective omnidirectional reflector that is transparent to normal, below-bandgap photons can be engineered between the junctions.

The authors acknowledge K. Emery and his team for solar cell measurements; S. Choi for spectral ellipsometry measurements; W. Olavarria, M. Young, A. Kibbler, and A. Duda for solar cell processing; and E. Yablonovich, R. King, and others from U.C. Berkeley and Spectrolab for helpful conversations. I. García holds an IOF grant from the People Programme (Marie Curie Actions) of the European Union's Seventh Framework Programme (FP7/2007-2013) under REA grant agreement n° 299878. Research was supported by the U.S. Department of Energy under Contract No. DE-AC36-08GO28308 with the National Renewable Energy Laboratory and funded by the Foundational Program to Advance Cell Efficiency (F-PACE).

[1]M. A. Steiner, J. F. Geisz, I. Garcia, D. J. Friedman, A. Duda, and S. R. Kurtz, J. Appl. Phys. **113**, 123109 (2013).
[2]O. D. Miller, E. Yablonovitch, and S. R. Kurtz, IEEE J. Photovolt. **2**, 303 (2012).
[3]B. M. Kayes, H. Nie, R. Twist, S. G. Spruytte, F. Reinhardt, I. C. Kizilyalli, and G. S. Higashi, in *Proceedings of the 37th IEEE Photovoltaic Specialist Conference, Seattle, WA* (IEEE, New York, 2011), p. 000004.
[4]I. García, J. Geisz, M. Steiner, J. Olson, D. Friedman, and S. Kurtz, in *Proceedings of the 38th IEEE Photovoltaic Specialists Conference, Austin, TX* (IEEE, New York, 2012), p. 002042.
[5]J. M. Olson, W. E. McMahon, and S. Kurtz, in *Proceedings of the 4th World Conference on Photovoltaic Energy Conversion, Waikoloa, HI* (IEEE, New York, 2006), p. 787.
[6]R. R. King, D. Bhusari, A. Boca, D. Larrabee, X. Q. Liu, W. Hong, C. M. Fetzer, D. C. Law, and N. H. Karam, Prog. Photovolt.: Res. Appl. **19**, 797 (2011).
[7]U. Rau, Phys. Rev. B **76**, 085303 (2007).
[8]M. A. Green, Prog. Photovolt. **20**, 472 (2012).
[9]W. Shockley and H. J. Queisser, J. Appl. Phys. **32**, 510 (1961).
[10]E. S. Toberer, A. C. Tamboli, M. Steiner, and S. Kurtz, in *Proceedings of the IEEE 38th Photovoltaic Specialists Conference, Austin, TX* (IEEE, New York, 2012), p. 001327.
[11]S. Roensch, R. Hoheisel, F. Dimroth, and A. W. Bett, Appl. Phys. Lett. **98**(25), 251113 (2011).
[12]C. T. Sah, R. N. Noyce, and W. Shockley, Proc. IRE **45**, 1228 (1957).
[13]S. C. Choo, Solid-State Electron. **11**, 1069 (1968).
[14]R. Hoheisel, F. Dimroth, A. W. Bett, S. R. Messenger, P. P. Jenkins, and R. J. Walters, Sol. Energy Mater. Sol. Cells **108**, 235 (2013).
[15]J. M. Olson, S. R. Kurtz, A. E. Kibbler, and P. Faine, Appl. Phys. Lett. **56**, 623 (1990).
[16]B. T. Cavicchi, D. D. Krut, D. R. Lillington, S. R. Kurtz, and J. M. Olson, in *Proceedings of the 22nd IEEE Photovoltaic Specialists Conference, Las Vegas, NV* (IEEE, New York, 1991), p. 63.
[17]S. R. Kurtz, J. M. Olson, K. A. Bertness, K. Sinha, B. McMahon, and S. Asher, in *Proceedings of the 25th IEEE Photovoltaic Specialists Conference, Washington D.C.* (IEEE, New York, 1996), p. 37.
[18]J. F. Geisz, S. R. Kurtz, M. W. Wanlass, J. S. Ward, A. Duda, D. J. Friedman, J. M. Olson, W. E. McMahon, T. Moriarty, and J. Kiehl, Appl. Phys. Lett. **91**, 023502 (2007).
[19]C. R. Osterwald, K. A. Emery, D. R. Myers, and R. E. Hart, in *Proceedings of the 21st IEEE Photovoltaic Specialist Conference, Kissimmee, FL* (IEEE, New York, 1990), p. 1067.
[20]T. Takamoto, E. Ikeda, H. Kurita, and M. Ohmori, Sol. Energy Mater. Sol. Cells **35**, 25 (1994).
[21]K. C. Reinhardt, Y. K. Yeo, P. H. Ostdiek, and R. L. Hengehold, J. Appl. Phys. **81**(8), 3700 (1997).
[22]F. W. Ragay, E. W. M. Ruigrok, and J. H. Wolter, in *Proceedings of the First World Conference on Photovoltaic Energy Conversion, Waikoloa, HI* (1994), p. 1934.
[23]D. G. Deppe, Appl. Phys. Lett. **56**, 370 (1990).
[24]M. A. Steiner, J. F. Geisz, R. C. Reedy, and S. Kurtz, in *Proceedings of the 33rd IEEE Photovoltaic Specialist Conference, San Diego, CA* (IEEE, New York, 2008).